# Effective passivation of black phosphorus against atmosphere by quasi-monolayer of F4TCNQ molecules

Cite as: Appl. Phys. Lett. 117, 061602 (2020); https://doi.org/10.1063/5.0015119 Submitted: 27 May 2020 . Accepted: 27 July 2020 . Published Online: 14 August 2020

- 🗓 Shitan Wang, Jialin Li, Yuan Zhao, Baoxing Liu, Pan Yuan, Junhua Wei, Jianhua Zhang, Haipeng Xie, Dongmei Niu,
- 🗓 Menggiu Long, and 🗓 Yongli Gao







View On

# ARTICLES YOU MAY BE INTERESTED IN

Current-induced torques in black phosphorus/permalloy bilayers due to crystal symmetry Applied Physics Letters 117, 062403 (2020); https://doi.org/10.1063/5.0013363

Light-emitting diodes with AIN polarization-induced buried tunnel junctions: A second look Applied Physics Letters 117, 061104 (2020); https://doi.org/10.1063/5.0015097

External quantum efficiency determined by combined thermal lens and photoluminescence spectroscopy techniques: Application to Ce<sup>3+</sup>:YAG

Applied Physics Letters 117, 061107 (2020); https://doi.org/10.1063/5.0011127





# Effective passivation of black phosphorus against atmosphere by quasi-monolayer of F4TCNQ molecules

Cite as: Appl. Phys. Lett. **117**, 061602 (2020); doi: 10.1063/5.0015119 Submitted: 27 May 2020 · Accepted: 27 July 2020 · Published Online: 14 August 2020







Shitan Wang, Dialin Li, Yuan Zhao, Baoxing Liu, Pan Yuan, Junhua Wei, Jianhua Zhang, Haipeng Xie, Dongmei Niu, Amengqiu Long, and Yongli Gao (2,4)

# **AFFILIATIONS**

<sup>1</sup>Hunan Key Laboratory for Super-microstructure and Ultrafast Process, School of Physics and Electronics, Central South University, Changsha, Hunan 410012, People's Republic of China

### **ABSTRACT**

Black phosphorus (BP) has drawn extensive attention due to its unique semiconducting properties, but the poor stability of BP greatly limits its practical device application. In this work, we have fabricated a passivation layer of quasi-monolayer 2,3,5,6-tetrafluoro-7,7,8,8-tetracyano-quinodimethane (F4TCNQ) on the BP simply by vacuum evaporation and annealing. The desirable air stability and strong interface charge transfer (ICT) of quasi-monolayer F4TCNQ/BP were confirmed with photoemission spectroscopy (PES) characterization. Density functional theory (DFT) calculations were also applied to further investigate the passivation mechanism, and the results show that the lone pair electrons in BP's valence band transfer to F4TCNQ molecules and were firmly localized due to the strong withdrawing ability of F4TCNQ, which greatly enhanced the energy barrier of electrons transfer to H<sub>2</sub>O and O<sub>2</sub> and hindered the further oxidation of phosphorus atoms. Meanwhile, a nearly Ohmic contact is formed across the F4TCNQ/BP interface which may greatly facilitate the carrier transport in BP based devices.

Published under license by AIP Publishing. https://doi.org/10.1063/5.0015119

Black phosphorus (BP) has been regarded as one of the most promising 2D materials and has attracted wide attention because of the unique and remarkable properties. BP has a thickness-dependent direct bandgap and a very high carrier mobility of 10<sup>3</sup> cm<sup>2</sup> v<sup>-1</sup> s<sup>-1</sup>, which combines the advantages of graphene and transition metal dichalcogenides and makes BP an excellent candidate for the traditional semiconductor fields. In addition, BP possesses unique anisotropic electrical, optical, mechanical, thermal, acoustical, and magnetic properties which are not only scientifically important but very likely to breed innovative devices.<sup>2–11</sup> With so many distinguished properties and high surface activity, BP has been demonstrated to be widely applicable in catalysis, biology, sensing, analysis, and other fields. 1-3,12-14 However, the high reactivity of the BP surface presents a major obstacle for the application of BP. The oxygen in the atmosphere can bond with surface phosphorus atoms to form a P-O bond by capturing the lone pair electrons of BP, and the formed phosphorus oxide can be further lifted off from the surface by the dragging of water molecules; thus, it leads to corrosion.

Both physical encapsulation and chemical passivation for the protection of BP have been developed theoretically and experimentally. Physically covering with inert two dimensional graphene,  $^{16}$  hexagonal boron nitride (h-BN),  $^{14}$  dense metal-oxide coatings,  $^{17,18}$  and polymers  $^{19}$  can block the ambient oxygen and water molecules from interacting with BP and prolong the BP's lifetime. However, the processability and some drawbacks of these approaches cannot be ignored. Most of chemical passivation approaches adopt a strategy that consumes the lone pair electrons by chemical reactions and constructing an inert outmost passivation layer to block the inner BP from degradation. This approach basically adopts materials containing functional groups or elements with higher electron affinity (EA), i.e., cluster Ni,  $\mathrm{Ag}^+$ , and Cl.  $^{20-22}$  A thick functional layer is always required for a desirable passivation effect, which may affect the intrinsic properties of BP or introduce additional contamination from chemical solvents.

In this article, we report our investigations on preparing a quasi-monolayer 2,3,5,6-tetrafluoro-7,7,8,8-tetracyanoquinodimethane

<sup>&</sup>lt;sup>2</sup>Department of Physics and Astronomy, University of Rochester, Rochester, New York 14627, USA

<sup>&</sup>lt;sup>a)</sup>Authors to whom correspondence should be addressed: mayee@csu.edu.cn, mqlong@csu.edu.cn, and ygao@pas.rochester.edu

(F4TCNQ) passivation layer for black phosphorus, which can significantly improve the air stability of BP. Combining photoemission spectroscopy (PES) and density functional theory (DFT) calculations, we investigated the interface electronic structures, charge transfer, and molecular adsorption of F4TCNQ/BP, and revealed the mechanism of desorption behavior and quasi-monolayer effectively passivation of F4TCNQ. Furthermore, such a quasi-monolayer protection layer is of significant value to the BP application since the very small thickness will not introduce much negative influence on the device performance.

As the electronic structure determined the chemical and physical activity of the materials, we first studied the influence of the F4TCNQ layer on BP electronic structures with ultra-violet photoemission spectrum (UPS) and x-ray photoemission spectrum (XPS) examination. The UPS demonstrates a significant charge transfer (CT) from BP to F4TCNQ molecules, as shown in Fig. 1. The evolutions of work function (WF) and Fermi level region as the deposition of F4TCNQ on BP are demonstrated in Figs. 1(a) and 1(b), respectively. Here, we replaced the usual mass thickness with the deposition time because the F4TCNQ molecules' desorption behavior on BP leads to the actual thickness deviating obviously from the thickness quartz crystal microbalance (QCM) monitored, which will be discussed later.

The WF, VBM, and sharp LEED pattern [inset of Fig. 1(b)] of cleaved BP are in accordance with previous studies. <sup>23,24</sup> The WF abruptly increased 0.63 eV at initial 3 min deposition and eventually stabilized at 5.52 eV after 96 min deposition. In Fig. 1(b), the VB peak height of pristine BP is much higher than VB-1 peak height. After 3 min deposition of F4TCNQ, the VB peak decreased significantly and is much lower than VB-1, indicating the electrons in VB have transferred to the F4TCNQ side. The 0.17 eV shift of VBM toward the Fermi level indicates the p-type doping effect on BP, which runs parallel to the VB decrease. With further deposition, the VB of BP gradually disappeared while there was still a weak VB-1 state at 2.08 eV (green dashed line), almost aligning with the HOMO-onset of F4TCNQ. The interface energy level alignment of F4TCNQ/BP is drawn in Fig. 1(c). Considering the 3.1 eV bandgap of F4TCNQ, the electron affinity (EA) of F4TCNQ is 4.57 eV from the UPS spectra, which is even

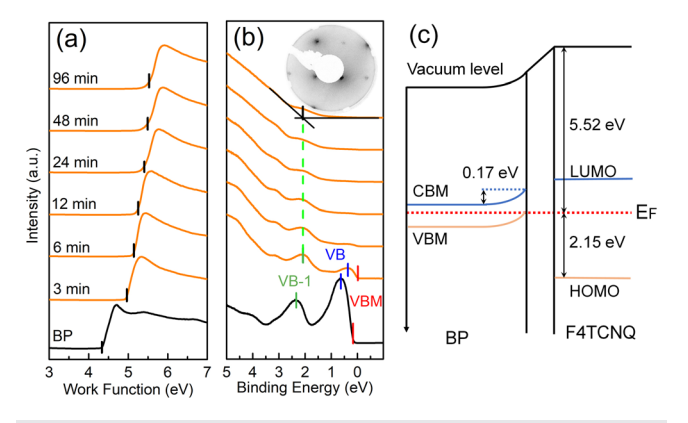


**FIG. 1.** The secondary electron cutoff edges (a) and HOMO (valence band) regions (b) evolution of pristine BP (black) and F4TCNQ on BP (orange) with various deposition times in the PES spectra; the inset of (b) is the low-energy electron diffraction (LEED) pattern of freshly cleaved BP. (c) The corresponding energy level alignment for the F4TCNQ/BP interface with the illustrative CT and charge accumulation. All the peaks have been normalized to the same height for clarity.

higher than the ionization potential (IP) of BP and facilitates the electrons transfer from BP's VB to the F4TCNQ molecule. This interface charge transfer (ICT) leads to the rapid disappearance of VB at very small amount of F4TCNQ deposition. The space charge layer is formed at the interface with electron accumulating at F4TCNQ side and holes at BP side. The band alignment demonstrates a nearly Ohmic contact, which is ideal for related semiconductor devices. In addition, DFT calculations show that ICT from BP to F4TCNQ molecule can dramatically enhance the p-type conductance of BP and further improve the performance of BP-based devices. This interface is the electron accumulation and the electron accumulation accumulation and the electron accumulation and the electron accumulation accumulation accumulation and the electron accumulation ac

To identify the detailed electron redistribution across the interfacial region and the chemical environment changes of each atom, we measured the core levels of P, N, and F elements with XPS. As shown in Fig. 2(a), the P  $2p_{3/2}$  and P  $2p_{1/2}$  peaks from intrinsic BP are located at  $130.04\,\text{eV}$  and  $130.85\,\text{eV}$  ( $P^0$ , blue peaks). The spin–orbit splitting separation between P  $2p_{3/2}$  and P  $2p_{1/2}$  is 0.81 eV, consistent with previous reports. 24,28-30 With 3 min deposition of F4TCNQ, a new component P<sup>+</sup> appeared at 129.73 eV (red peak), which originates the positive-charged interfacial BP layer. The lower binding energy of the interface component P+ is consistent with the p-type doping effect on BP in the UPS examination. Due to the ICT from BP to F4TCNQ, a hole accumulation layer is formed on BP side, and thus p-type doping effect and a new P+ component are shown in UPS and XPS, respectively. With further deposition, intrinsic BP is gradually covered by the positive-charged BP layer and F4TCNQ film, and the P<sup>+</sup> peak takes up more proportion due to the limitation of photoemission detection depth. The N 1s spectra showed a similar evolution [Fig. 2(b)]; there are three components N<sup>-</sup> (397.67 eV), N<sup>0</sup> (399.18 eV), and N<sup>s</sup> (401.75 eV) in N 1s spectra after initial 3 min deposition of F4TCNQ, which can be assigned to negative-charged F4TCNQ molecules, electroneutral F4TCNQ molecules at interface, and the shakeup processes, respectively.<sup>31,32</sup> Further deposition results in a continuous increase in N<sup>0</sup> and N<sup>s</sup> components' intensity and gradual decrease in the N<sup>-</sup> peak. There are two components in the F 1s peak located at 686.91 eV (F<sup>-</sup>, yellow peak) and 687.64 eV (F<sup>0</sup>, violet peak), 32-34 which derive from negative-charged and electroneutral F4TCNQ molecules, respectively. These evolutions of P 2p, N 1s, and F 1s core levels are in step with each other. The ICT caused by F4TCNQ molecules has an

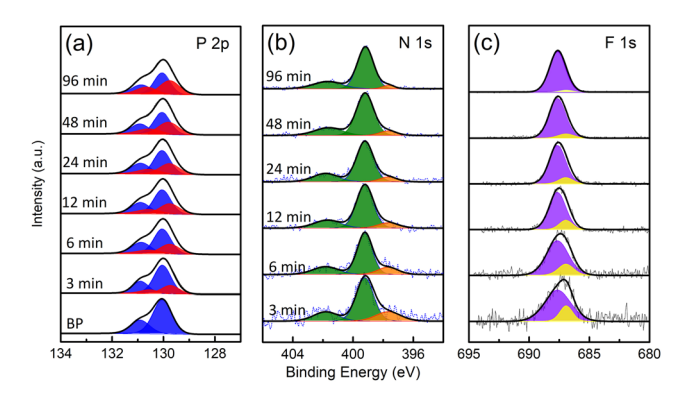


**FIG. 2.** The core levels evolution of (a) P 2p, (b) N 1s, and (c) F 1s as a function of F4TCNQ film deposition time on BP. All the peaks have been normalized to the same height for clarity.

obvious modulation effect on the Fermi level, resulting in a p-type doping effect on BP.

In order to get the quantitative charge redistribution across the interface between F4TCNQ and BP, DFT calculations were performed. Figures 3(a) and 3(b) show the optimized adsorption configuration of the F4TCNQ molecule on BP, which has lower adsorption energy and layer height than other adsorption configurations (Table S1 and Fig. S1). The charge distribution shows that the CT from BP to 1 ML F4TCNQ molecules [Fig. 3(c)] is 0.91 e, indicating that the F4TCNQ molecules have high electron withdrawing ability. The yellow region and cyan region denote the charge accumulation and charge depletion. The total CT of few layer F4TCNQ on BP (Fig. S2) is almost same with that of monolayer-F4TCNQ/BP. For bilayer F4TCNQ on BP, 0.70 e of the total 0.90 e from BP locates in the bottom layer F4TCNQ molecules and only 0.20 e transfers to the top layer. For trilayer-F4TCNQ/BP system, 0.73 e of the total 0.86 e locates in the bottom layer F4TCNQ, only 0.04 e and 0.09 e transfers to middle layer F4TCNQ and top layer F4TCNQ, respectively. In the above three systems, the transferred electrons from BP are mainly localized at the bottom layer F4TCNQ molecules, indicating that the bottom layer has more stable adsorption and a stronger drawback ability for the lone pair electrons in BP. The insignificant CT in upper layer F4TCNQ, specifically for the 3 ML system, shows a much weaker interaction with BP, which is a hint of the desorption of the F4TCNQ film.

As aforementioned, we noticed the mass thickness read from the QCM monitor deviated from the thickness estimated by the XPS intensity. During the step by step film deposition and XPS measurement, we found the core level peak intensity of the F4TCNQ film with

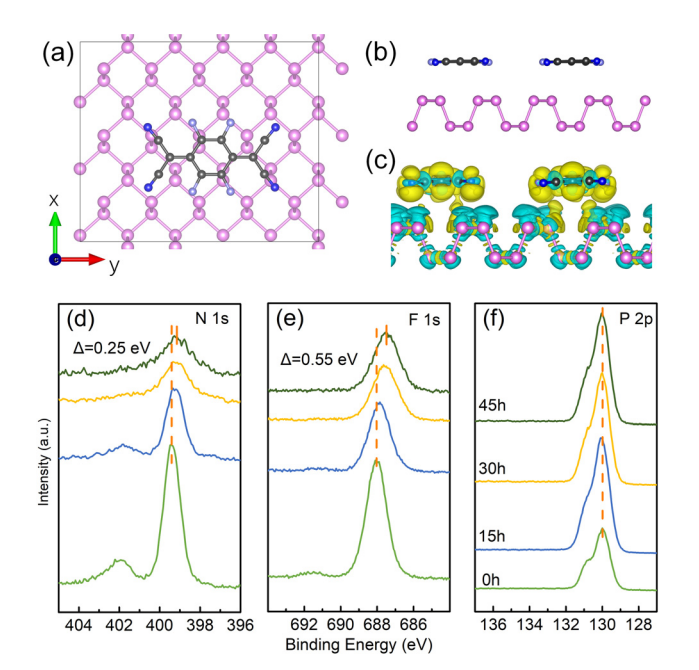


**FIG. 3.** The adsorption configuration [(a) and (b)] and charge density difference (c) of monolayer F4TCNQ molecules on BP. The yellow and cyan volumes in (c) represent electron accumulation and depletion, respectively. The intensity evolution of (d) N 1s, (e) F 1s, and (f) P 2p for 10 nm F4TCNQ on BP as a function of desorption time.

QCM thickness of 9.6 nm is only 10<sup>3</sup>, which is about an order of magnitude less than usual spectra intensity of other organic films. To find out if there is desorption of the upper layer F4TCNQ molecules, we prepared a 10 nm F4TCNQ film on BP with a deposition rate of 1 nm/ min, which is much more rapid than usual deposition rate of 0.1 nm/ min, and examined the peak intensities of core levels (P 2p, N 1s, and F 1s) after 0 h, 15 h, 30 h, and 45 h, as shown in Figs. 3(d)-3(f). As shown in Figs. 3(d) and 3(e), the intensities of N 1s and F 1s peaks from F4TCNQ decreased greatly, while the BP's P 2p peak intensity increases significantly in the initial 15 h, reflecting the fast desorption of the upper layer F4TCNQ molecules. It can be seen from the intensity evolutions P 2p, N 1s, and F 1s peaks that the desorption behavior is significant in the first 15 h. After 30 h, all the three peaks of P 2p, F 1s, and N 1s show negligible change, manifesting that the desorption is much slower or even ceased. After 45 h desorption, the positions of F 1s and N 1s peaks shift 0.25 eV and 0.55 eV to low binding energy side, which approach to the corresponding negative-charged interface components in Fig. 2. These changes can be ascribed to that the desorption behavior of upper layer F4TCNQ and the residual signals after 45 h mainly come from the interfacial F4TCNQ molecules, indicating that the interfacial molecules cannot desorb from the BP. The similar desorption behaviors of F4TCNQ have also been reported in previous studies; meanwhile, F4TCNQ molecules have conspicuous diffusivity on organic films even at room temperature, which is related to the organic film structure and intermolecular interaction.

The AFM characterization was performed to clarify the thickness of the stably adsorbed F4TCNQ film. No apparent terraces were found, and the surface showed a typical amorphous morphology. We also performed LEED investigations and found no pattern, which is consistent with the amorphous morphology image of AFM (Fig. S3). It can be deduced from the absence of terraces that the residual F4TCNQ film might be an amorphous quasi-monolayer one after sufficient desorption in the vacuum. We also estimated the thickness of the stably adsorbed film with the photoelectrons intensity and found a film thickness close to monolayer. More specifically, the photoelectrons intensity I(d) for a uniform F4TCNQ film with thickness of d nm can be expressed by the following equation:

$$I(d) = I_{\infty}[1 - \exp(-d/\lambda \sin \theta)]\sin \theta, \tag{1}$$

where  $I_{\infty}$  are the photoelectrons' intensity for the film which is thicker than detection depth;  $\lambda$  and  $\theta$  are mean free path and emission angle of the photoelectrons, respectively. The emission angle  $\theta$  is 90° in our measurement, and the  $\lambda$  can be estimated by the universal curve for the electron inelastic mean free path. Thus, it can be calculated that the value of  $d_2$  is 0.57 nm, which is close to the thickness of quasi-monolayer F4TCNQ. The 0.57 nm thickness calculation runs parallel with the inference that only the interfacial layer is left for the stable adsorption configuration.

To further understand this desorption behavior of F4TCNQ, we calculated the dissociation energy  $(E_d)$  of each single layer of F4TCNQ from the first to third layer. The  $E_d$  of interfacial F4TCNQ molecule on BP is 1.83 eV, while that of the second layer for the bilayer F4TCNQ system is 1.45 eV. The higher  $E_d$  of the interfacial layer indicates a more stable adsorption configuration, which agrees with the XPS results in Fig. 3. For the trilayer F4TCNQ on BP, the  $E_d$  of the upmost layer is about 0.87 eV and even lower than that of bulk F4TCNQ molecules (1.19 eV). The dramatically decreasing  $E_d$  indicates an unstable

adsorption configuration of the upper layer F4TCNQ molecule, which is the key factor of desorption behavior. The desorption of F4TCNQ can be attributed to the CT from BP to F4TCNQ. Apparently, the charge distribution in F4TCNQ molecule is uneven, and the F atoms and cyan groups are negatively charged, while the aromatic ring is positively charged due to the difference of electrophilic ability [Fig. S7(a)]. The electrostatic attraction between the oppositely charged groups forms the main contribution of the intermolecular  $\pi$ - $\pi$  interaction, resulting in a stable offset adsorption configuration. The original intramolecular charge distribution of F4TCNQ is broken when the F4TCNQ molecules are totally negatively charged, as shown in Fig. S7. Therefore, the electrostatic  $\pi$ - $\pi$  interaction will be significantly weaken, further leading to the decrease in  $E_d$  and desorption of F4TCNQ. As the  $E_d$  of the monolayer and bilayer F4TCNQ with BP is as high as 1.83 eV and 1.45 eV respectively, the desorption will be greatly depressed when there is only 1 or 2 layers left. Thereby, this desorption behavior provides us an efficient method to prepare a quasi-monolayer F4TCNQ passivation layer on BP. To obtain a stable adsorption configuration of quasimonolayer F4TCNQ, we simply evaporated a thick film of F4TCNQ to BP and then annealed it at 90 °C for 2 h.

Although the thus-prepared passivation layer has only small amount of F4TCNQ molecules adhered to the BP surface, a remarkable anti-degradation effect was observed in the following exposure test. Because of the surface sensitivity and analytical nature, XPS is particularly suitable for investigating degradation induced by ambient factors.<sup>28-30,39</sup> Quasi-monolayer F4TCNQ/BP as well as cleaved bare BP was exposed to environmental atmosphere, and their anti-degradation effect was checked with XPS, as illustrated in Figures 4(a)-4(c). The bare BP is highly sensitive to the air environment, and a visible phosphorus oxide component appears at 134.5 eV with only 3 h of air exposure. With the increase in exposure time, the phosphorus oxide component intensity is greatly enhanced and the intrinsic P 2p component shows a slight shift of 0.17 eV with the formation of phosphorus oxides, which can be attributed to the CT from BP to O2 molecules. In contrast, the P 2p peak of quasi-monolayer-F4TCNQ/BP does not show any shift or any new components even with up to 3 days air exposure

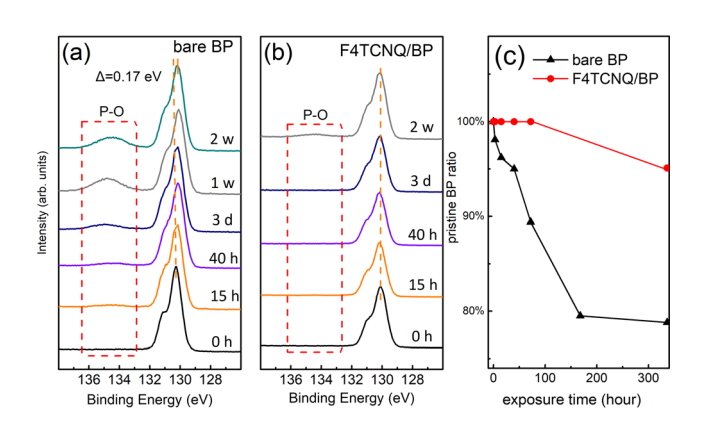


**FIG. 4.** The anti-degradation effect of air exposure on BP and BP passivated with quasi-monolayer F4TCNQ molecules. The evolution of P 2p core level XPS spectra of (a) bare BP and (b) BP covered with quasi-monolayer F4TCNQ as a function of air exposure levels. All the peaks have been normalized to same intensity for clarity. (c) The degradation evolutions of bare BP (black curve) and quasi-monolayer-F4TCNQ/BP (red curve).

(50% humidity), which implies remarkable stability of quasi-monolayer F4TCNQ/BP. Figure 4(c) quantitatively illustrates the proportion of the pristine BP component in bare BP and quasi-monolayer-F4TCNQ covered BP with increase in air exposure time. As we can see, the degradation of bare BP is very rapid, and more than 20% pristine BP has been oxidized to the phosphorus oxides within 1 week. However, the quasi-monolayer-F4TCNQ/BP shows outstanding stability and can keep pristine for several days. 95% of BP was well protected from degradation even after 2 weeks exposure, which is much better than the 78% of bare BP. AFM measurements also confirm the passivation effect of F4TCNQ, as shown in Fig. S4. After 24 h ambient exposure, many oxidized bubbles appeared on the originally smooth BP surface. In contrast, the surface morphology of F4TCNQ-covered BP showed no observable change after exposure. Both the XPS and AFM manifest that the F4TCNQ indeed markedly improved the stability of BP in ambient.

In order to further understand the anti-degradation mechanism of F4TCNQ on BP, charge density differences of systems that O<sub>2</sub> + H<sub>2</sub>O cluster adsorbed on BP covered with/without F4TCNQ molecules were performed. For the bare BP system, there is significant CT (0.28 e) from BP to O<sub>2</sub> through H<sub>2</sub>O, which induces the formation of O<sub>2</sub><sup>-</sup> anions and lower reaction energy barrier of oxidation. The formed P-O bond is pulled by H<sub>2</sub>O with the hydrogen bonding, leading to further degradation of BP. 15 In contrast, for 1 ML and 2 ML F4TCNQ covered BP, the charge accumulation region is firmly localized at the F4TCNQ layer and few electrons transfer to  $O_2 + H_2O$  cluster. The F4TCNQ molecule shows stronger electron withdrawing ability than O2 + H2O cluster (Fig. 5), which greatly suppresses the reaction between oxygen molecules and phosphorus atoms. In addition, F4TCNQ has been used as a passivation layer of perovskite because it has desirable hydrophobicity that may keep the underlying surface from corrosion caused by moisture. 40,41 Our hydrophobicity examination with XPS also shows that F4TCNQ can provide BP with desirable hydrophobicity in a moisture environment (Figs. S5 and S6), which should play a role in the passivation of BP. These results demonstrate that quasi-monolayer F4TCNQ can reduce CT to oxygen and partly insulate water molecules, which are the crucial factors for long term stability of the underneath BP.

In summary, we have presented an efficient way to prepare a quasi-monolayer F4TCNQ protection film for BP by vacuum

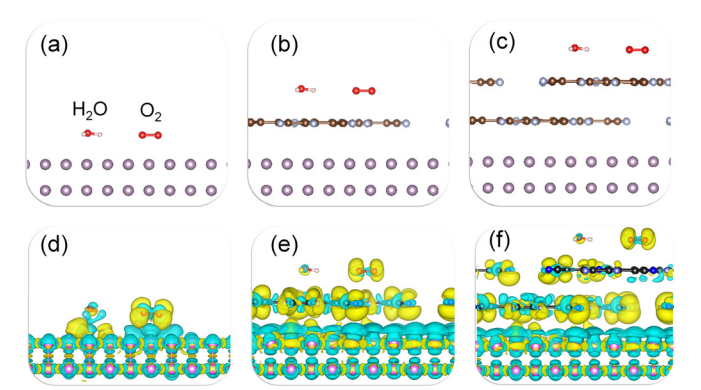


**FIG. 5.** The adsorption configurations [(a)–(c)] and charge density differences [(d)–(f)] of  $O_2+H_2O$  cluster on bare BP, 1 ML F4TCNQ/BP, and 2 ML F4TCNQ/BP, respectively. The yellow and cyan volumes represent electron accumulation and depletion.

evaporating and annealing, and have also revealed the passivation effect and mechanism with PES measurements and DFT calculations. These results showed that F4TCNQ can strongly withdraw and localize the electrons from the BP's VBM to effectively passivate the chemical activity of BP, achieving up to 2 weeks stability of BP in the air exposure test. Meanwhile, we also found the obvious desorption behavior of F4TCNQ on BP, which actually facilitates the preparation of a quasi-monolayer F4TCNQ film. In addition, the heterojunction is as thin as only quasi-monolayer and has a nearly Ohmic contact at the interface, which is of great value for the applications of BP based devices.

See the supplementary material for the additional DFT calculations results and the methods of experiments and DFT calculations.

This work was supported by the National Key Research and Development Program of China (Grant No. 2017YFA0206602) and National Natural Science Foundation of China (Grant No. 51802355). Y.G. acknowledges the support from the National Science Foundation DMR 1903962. S.W. was supported by Hunan Provincial Innovation Foundation For Postgraduate (Grant No. CX2018B037). H.X. acknowledges the support by the Natural Science Foundation of Hunan Province (Grant No. 2018JJ3625). The authors acknowledge the assistance provided by Mr. Yuquan Liu, Jia Liu, and Yangyang Zhang.

### **DATA AVAILABILITY**

The data that support the findings of this study are available from the corresponding authors upon reasonable request.

# **REFERENCES**

- <sup>1</sup>L. Li, Y. Yu, G. J. Ye, Q. Ge, X. Ou, H. Wu, D. Feng, X. H. Chen, and Y. Zhang, Nat. Nanotechnol. **9**, 372 (2014).
- <sup>2</sup>A. S. Rodin, A. Carvalho, and A. H. Castro Neto, Phys. Rev. Lett. **112**, 176801 (2014).
- <sup>3</sup>H. Yuan, X. Liu, F. Afshinmanesh, W. Li, G. Xu, J. Sun, B. Lian, A. G. Curto, G. Ye, Y. Hikita, Z. Shen, S. C. Zhang, X. Chen, M. Brongersma, H. Y. Hwang, and Y. Cui, Nat. Nanotechnol. 10, 707 (2015).
- <sup>4</sup>Y. W. Wang, S. Liu, B. W. Zeng, H. Huang, J. Xiao, J. B. Li, M. Q. Long, S. Xiao, X. F. Yu, Y. L. Gao, and J. He, Nanoscale **9**, 4683 (2017).
- <sup>5</sup>J. Zhang, X. Yu, W. Han, B. Lv, X. Li, S. Xiao, Y. Gao, and J. He, Opt. Lett. **41**, 1704 (2016).
- <sup>6</sup>Y. Wang, G. Huang, H. Mu, S. Lin, J. Chen, S. Xiao, Q. Bao, and J. He, Appl. Phys. Lett. 107, 091905 (2015).
  <sup>7</sup>S. Zheng, F. Wu, Z. Feng, R. Zhang, Y. Xie, Y. Yu, R. Zhang, O. Li, I. Liu, W.
- <sup>7</sup>S. Zheng, E. Wu, Z. Feng, R. Zhang, Y. Xie, Y. Yu, R. Zhang, Q. Li, J. Liu, W. Pang, H. Zhang, and D. Zhang, Nanoscale 10, 10148 (2018).
- <sup>8</sup>Z. Luo, J. Maassen, Y. Deng, Y. Du, R. P. Garrelts, M. S. Lundstrom, P. D. Ye, and X. Xu, Nat. Commun. 6, 8572 (2015).
- <sup>9</sup>H. Jang, J. D. Wood, C. R. Ryder, M. C. Hersam, and D. G. Cahill, Adv. Mater. 27, 8017 (2015).
- <sup>10</sup>L. Kou, C. Chen, and S. C. J. J. o P. C. L. Smith, J. Phys. Chem. Lett. 6, 2794 (2015).
- <sup>11</sup>V. Tran, R. Soklaski, Y. Liang, and L. Yang, Phys. Rev. B **89**, 235319 (2014).
- <sup>12</sup>M. V. Kamalakar, B. N. Madhushankar, A. Dankert, and S. P. Dash, Small 11, 2209 (2015).
- <sup>13</sup>P. Li, D. Zhang, J. Liu, H. Chang, Y. e Sun, and N. Yin, ACS Appl. Mater. Interfaces 7, 24396 (2015).

- <sup>14</sup>R. A. Doganov, E. C. T. O'Farrell, S. P. Koenig, Y. Yeo, A. Ziletti, A. Carvalho, D. K. Campbell, D. F. Coker, K. Watanabe, T. Taniguchi, A. H. C. Neto, and B. Özyilmaz, Nat. Commun. 6, 6647 (2015).
- <sup>15</sup>Q. Zhou, Q. Chen, Y. Tong, and J. Wang, Angew. Chem., Int. Ed. Engl. 55, 11437 (2016).
- 16 A. Avsar, I. J. Veramarun, J. Y. Tan, K. Watanabe, T. Taniguchi, A. H. C. Neto, and B. Ozyilmaz, ACS Nano 9, 4138 (2015).
- <sup>17</sup>R. Galceran, E. Gaufres, A. Loiseau, M. Piquemal-Banci, F. Godel, A. Vecchiola, O. Bezencenet, M. B. Martin, B. Servet, F. Petroff, B. Dlubak, and P. Seneor, Appl. Phys. Lett. 111, 243101 (2017).
- <sup>18</sup>J. Na, Y. T. Lee, J. A. Lim, D. K. Hwang, G. Kim, W. K. Choi, and Y. Song, ACS Nano 8, 11753 (2014).
- <sup>19</sup>Y. Zhao, H. Wang, H. Huang, Q. Xiao, Y. Xu, Z. Guo, H. Xie, J. Shao, Z. Sun, W. Han, X. F. Yu, P. Li, and P. K. Chu, Angew. Chem. Int. Ed. Engl. 55, 5003 (2016).
- <sup>20</sup>Z. Guo, S. Chen, Z. Wang, Z. Yang, F. Liu, Y. Xu, J. Wang, Y. Yi, H. Zhang, L. Liao, P. K. Chu, and X.-F. Yu, Adv. Mater. 29, 1703811 (2017).
- <sup>21</sup>M. Caporali, M. Serrano-Ruiz, F. Telesio, S. Heun, G. Nicotra, C. Spinella, and M. Peruzzini, Chem. Commun. 53, 10946 (2017).
- <sup>22</sup>B. Yang, B. Wan, Q. Zhou, Y. Wang, W. Hu, W. Lv, Q. Chen, Z. Zeng, F. Wen, J. Xiang, S. Yuan, J. Wang, B. Zhang, W. Wang, J. Zhang, B. Xu, Z. Zhao, Y. Tian, and Z. Liu, Adv. Mater. 28, 9408 (2016).
- 23L. H. De Lima, L. Barreto, R. Landers, and A. De Siervo, Phys. Rev. B 93, 035448 (2016).
- <sup>24</sup>B. Liu, H. Xie, Y. Liu, C. Wang, S. Wang, Y. Zhao, J. Liu, D. Niu, H. Huang, and Y. Gao, J. Magn. Magn. Mater. 499, 166297 (2020).
- 25X. Liu, S. Yi, C. Wang, C. Wang, and Y. Gao, J. Appl. Phys. 115, 163708 (2014).
- <sup>26</sup>L. Li, C. Wang, C. Wang, S. Tong, Y. Zhao, H. Xia, J. Shi, J. Shen, H. Xie, X. Liu, D. Niu, J. Yang, H. Huang, S. Xiao, J. He, and Y. Gao, Org. Electron. 65, 162 (2019).
- <sup>27</sup>Y. He, F. Xia, Z. Shao, J. Zhao, and J. Jie, J. Phys. Chem. Lett. **6**, 4701 (2015).
- <sup>28</sup>X. Zhu, T. Zhang, D. Jiang, H. Duan, Z. Sun, M. Zhang, H. Jin, R. Guan, Y. Liu, M. Chen, H. Ji, P. Du, W. Yan, S. Wei, Y. Lu, and S. Yang, Nat. Commun. 9, 4177 (2018).
- <sup>29</sup> X. Liu, Y. Bai, J. Xu, Q. Xu, L. Xiao, L. Sun, J. Weng, and Y. Zhao, Adv. Sci. 6, 1901991 (2019).
- <sup>30</sup>S. J. R. Tan, I. Abdelwahab, L. Chu, S. M. Poh, Y. Liu, J. Lu, W. Chen, and K. P. Loh, Adv. Mater. **30**, 1704619 (2018).
- <sup>31</sup>W. Chen, S. Chen, D. Qi, X. Gao, and A. T. S. Wee, J. Am. Chem. Soc. 129, 10418 (2007).
- <sup>32</sup>L. Khalil, D. Pierucci, E. Papalazarou, J. Chaste, M. G. Silly, F. Sirotti, M. Eddrief, L. Perfetti, E. Lhuillier, and A. Ouerghi, Phys. Rev. Mater. 3, 084002 (2019).
- 33B. He, T. W. Ng, M. F. Lo, C. S. Lee, and W. Zhang, ACS Appl. Mater. Interfaces 7, 9851 (2015).
- <sup>34</sup>Y. J. Hsu, Y. L. Lai, C. H. Chen, Y. C. Lin, H. Y. Chien, J. H. Wang, T. N. Lam, Y. L. Chan, D. H. Wei, H. J. Lin, and C. T. Chen, J Phys. Chem. Lett. 4, 310 (2013).
- 35W. Gao and A. Kahn, J. Appl. Phys. 94, 359 (2003).
- <sup>36</sup>S. Duhm, I. Salzmann, B. Bröker, H. Glowatzki, R. L. Johnson, and N. Koch, Appl. Phys. Lett. **95**, 093305 (2009).
- <sup>37</sup>J. Li, C. W. Rochester, I. E. Jacobs, S. Friedrich, P. Stroeve, M. Riede, and A. J. Moule, ACS Appl. Mater. Interfaces 7, 28420 (2015).
- 38M. P. Seah and W. A. Dench, Surf. Interface Anal. 1, 2 (1979).
- <sup>39</sup>Z. Hu, Q. Li, B. Lei, Q. Zhou, D. Xiang, Z. Lyu, F. Hu, J. Wang, Y. Ren, R. Guo, E. Goki, L. Wang, C. Han, J. Wang, and W. Chen, Angew. Chem. Int. Ed. Engl. 56, 9131 (2017).
- <sup>40</sup>H. Kwon, J. W. Lim, J. Han, L. N. Quan, D. Kim, E. S. Shin, E. Kim, D. W. Kim, Y. Y. Noh, I. Chung, and D. H. Kim, Nanoscale 11, 19586 (2019).
- <sup>41</sup>G. Gong, N. Zhao, J. Li, F. Li, J. Chen, Y. Shen, M. Wang, and G. Tu, Org. Electron. 35, 171 (2016).